

## Experimental study of materials for the filtration of the intake air of the internal combustion engine of a motor vehicle

### ARTICLE INFO

*Fiber composite materials show more favorable filtration properties in terms of filtration efficiency and accuracy, as well as dust absorption. Experimental tests of standard filtration materials based on cellulose, polyester, glass microfiber, cotton and polyester nonwoven fabrics were performed using an original method. Two composite beds consisting of three layers of standard materials were designed using a novel method: K1 (polyester-glass-microfiber-cellulose) and K2 (cellulose-glass-microfiber-cellulose), and determined their effectiveness, the size of dust grains in the cleaned air and the unit dust absorption. It was shown that the K1 composite has high ( $d_{pmax} = 1.5\text{--}3\ \mu\text{m}$ ) filtration accuracy, high initial filtration efficiency (99.8%), which shortens the preliminary stage, and extends to 96–98% the duration of the main stage of the filtration process. The K1 composite achieved more than twice the dust mass loading value ( $k_{dK1} = 148.9\ \text{g/m}^2$ ), compared to other standard materials. These are parameters that are essential for filter design in automotive technology and can only be obtained through empirical testing. Knowing them will make it possible to make an air filter design with smaller dimensions or to extend vehicle mileage.*

Received: 4 December 2023

Revised: 27 December 2023

Accepted: 7 January 2024

Available online: 14 February 2024

Key words: engine, air filtration, fiber filtration materials, composite materials, air filter characteristics, vehicle mileage

This is an open access article under the CC BY license (<http://creativecommons.org/licenses/by/4.0/>)

### 1. Introduction

Along with the air sucked in by the internal combustion engines of motor vehicles, significant amounts of pollutants are sucked in, which accumulate on the road surface and are carried into the atmosphere as a result of vehicle traffic or wind gusts. The composition of road pollutants is wide and varied. The primary component is mineral dust carried by the wind from the nearby environment, where it was generated by field, road, or construction work. It is also dust that has been carried by the wind from large sandy and desert areas, as well as volcanic ash fallout. Industrial production, the operation of open-pit mines is the cause of emissions of a very large amount of dust [50]. The main components of mineral dust are silica ( $\text{SiO}_2$ ), the mass proportion of which in the dust is in the range of 65–97%, and alumina  $\text{Al}_2\text{O}_3$ , the mass content of which in the dust is 5–18%. Other components are oxides of various metals:  $\text{F}_2\text{O}_3$ ,  $\text{CaO}$ ,  $\text{MgO}$  and organic components [39].

Another component of road dust is plant and tree inflorescence elements, pollen, insect fragments, animal dander and other biological materials [2, 24]. Significant amounts of dust are emitted into the atmosphere during the work of harvesting crops and other crops [20]. The use of motor vehicles is mainly "non-motor" pollutants, i.e. those generated by the abrasion process in friction pairs: brake disc-friction lining, clutch disc-pressure plate [41, 43], as well as by the abrasion of the tire tread against the road surface [19, 22, 36, 47]. The engine's exhaust system is mainly a source of soot, which is a product of incomplete combustion of fuel, as well as products of abrasive wear of the engine's metal surfaces, which form the piston-ring-cylinder or journal-pan associations. During the operation of vehicles in winter conditions, salt and sand, products used for de-icing roads, may be present on the road surface. The accumulation of dirt on the road surface, which is lifted to a consid-

erable height by vehicles or wind, is called road dust in the literature [9, 13, 14].

Passenger car engines operating at rated conditions draw in an air flow of 180–500 kg/h from the environment, depending on the engine's displacement and its speed. Truck engines require 1100–1600 kg/h of air for operation, and vehicle engines require more than 7500 kg/h of ambient air.

In the inlet air stream of an internal combustion engine, there can be significant amounts of impurities, mainly mineral dust, which is the primary component of dust. The presence of hard  $\text{SiO}_2$  and  $\text{Al}_2\text{O}_3$  grains, which are characterized by a hardness of 7 and 9, respectively, on the ten-degree Mohs scale [40], is the main cause of wear of mating parts: piston sealing and scraping rings and cylinder liners, crankshaft and camshaft plain bearings, valve stems and their guides.

The available literature shows that abrasive wear on the surfaces of engine components and, as a result, a reduction in engine performance, durability and reliability is caused largely by the improper quality of air supplied to engine cylinders [1, 30, 45]. Abrasive wear of engine components is determined by the hardness, but also by the size of dust particles, their irregular shape, and sharp edges. It is accepted in the literature that dust particles with sizes in the range of 1–40  $\mu\text{m}$  are the primary cause of wear on the two moving surfaces, but dust grains having a size of 5–20  $\mu\text{m}$  are the most aggressive [4, 6, 7]. The prevailing view is that dust grains between two mating engine components whose diameter  $d_p$  is equal to the thickness of the oil film  $h_{min}$  at any given time are the cause of wear.

The mass of dust that is in the engine intake air stream depends on the dust concentration in the air, which can take on varying values depending on the conditions of vehicle use. The lowest values of dust concentration in the air (from 0.00045  $\text{g/m}^3$  to 0.1  $\text{g/m}^3$ ) are found on highways [3], the

highest (within  $0.001\text{--}10\text{ g/m}^3$ ) when vehicles are used on sandy roads [16]. During tracked vehicle traffic in desert conditions, dust concentrations in the air reach values of up to about  $20\text{ g/m}^3$  [4, 10, 38].

Not all dust grains that enter the engine cylinders with the air have a destructive effect on engine durability. It is estimated that about 10–20% of the dust that penetrates the engine is retained on the oil-wetted walls of the cylinder liner and comes into contact with the surface of the piston and piston rings, causing their abrasive wear. About 30% of the contaminants that enter the engine can escape with the exhaust in the same form into the exhaust system. Mineral dust grains, whose melting points are much lower than the peak temperature (about  $2500^\circ\text{C}$ ) in the cylinder during fuel combustion, melt, after which they can enter with the exhaust gas into the exhaust system in the form of droplets and deposit on the walls of the catalytic layer. This creates an additional layer that impedes its operation [5].

Dust grains that enter with the air can retain and deposit on the measuring element (wire or layer thermo anemometer) of the airflow meter, forming an insulating layer that impedes heat dissipation from the measuring element. Deposition is facilitated by moisture and oil mist from the crankcase venting system, which penetrates the measuring element of the flow meter as a result of backflows in the intake system. Isolation of the measuring element, which is incompletely cooled by the flowing air stream, causes: underestimation of the voltage signal  $U_w$  of the air flow meter, so that the controller dispenses a lower mass of fuel to create the fuel-air mixture, resulting in lower engine torque and power values. In addition, hard sharp-edged dust grains ( $\text{SiO}_2$ ,  $\text{Al}_2\text{O}_3$ ) moving at high speed hit the stationary measuring element (heater wire) causing scratches on its surface, resulting in its weakening or even complete destruction.

Wear and tear on the components of the piston-piston-ring-cylinder association results in an increase in clearance, which is the cause of increased charge blow-off into the crankcase during the compression stroke. The loss of working medium mass from the cylinders caused by this phenomenon results in a decrease in pressure at the end of the compression stroke, resulting in a decrease in engine torque and power and an increase in exhaust emissions [21, 33, 48, 51]. Excessive clearances in the P-PR-C linkage increase the flow of hot exhaust gases through the labyrinth ring spaces into the crankcase. This phenomenon increases the temperature of the lubricating oil and decreases its viscosity, which can lead to excessive wear and seizure of the engine. Exhaust fumes in the crankcase contaminate the oil with soot, increase its temperature and viscosity. This can negatively affect engine life and vehicle reliability [34].

Modern passenger car engines, because that they are used mostly on paved roads with low dust concentrations in the air, are equipped with single-stage filters with a pleated paper insert. In trucks and special vehicles, since their use is mostly on paved roads with a high concentration of dust in the air, it is necessary to use two-stage filters. This is an assembly: an inert filter and a cylindrical filter element arranged in series behind it, shaped from pleated

paper or a composite of filter materials, such as: polyester, microglass and cellulose [37].

The placement of an air filter in the engine intake system is a necessity. However, there are negative effects of its presence in the form of a pressure drop, which leads to additional energy losses in the form of reduced torque and a drop in engine power [31, 42]. In addition, in passenger cars, due to the small space around the engine, there are difficulties in placing a filter with a sufficiently large area of filter material. Therefore, it is expedient to use materials with high surface absorption, low flow resistance and high efficiency and accuracy of dust particle filtration. Such possibilities are provided by fibrous composite filter materials, the filtration properties of which will be analyzed in this study.

## 2. Properties of composite filter beds

Cellulose-based fiber filter media are widely used in the air filtration systems of modern vehicle and machine drive engines and for indoor air filtration [25, 35]. Cellulose filter media, whose structure is formed by fibers with diameters of  $10\text{--}20\text{ }\mu\text{m}$ , are characterized by high durability compared to some other filter materials. However, their filtration efficiency and accuracy are not always satisfactory, especially during the first (initial) period of filtration, which is characterized by the fact that at the start of the filtration process there is a low-efficiency  $\varphi_f$  and filtration accuracy  $d_{p_{\text{max}}}$ , as well as low flow resistance  $\Delta p_f$  [12]. However, as the filtration process proceeds, the mass of dust retained on the filter bed increases. There is an increase in filtration efficiency  $\varphi_f$ , filtration accuracy  $d_{p_{\text{max}}}$  and flow resistance  $\Delta p_f$ . According to the research presented in the paper [12], the initial efficiency of the bed made of cellulose is  $\varphi_{f0} = 96.3\%$ . The criterion for completing the initial filtration period was that the bed achieved a filtration efficiency of  $\varphi_f = 99.5\%$ . This condition was obtained at a mass loading of dust of  $k_d = 110.7\text{ g/m}^2$ . This is half of the total operating time of the cartridge. During this time, there were maximum dust grains of  $d_{p_{\text{max}}} = 10\text{--}28\text{ }\mu\text{m}$  in the air behind the tested cartridge. Under the conditions of actual engine operation, these are the grains that cause the most wear on mating components.

Engine inlet air filter materials are required to have a filtration efficiency of more than 99.5% and a particle filtration accuracy of more than  $5\text{ }\mu\text{m}$  over the entire operating range and long service intervals. Because cellulosic filter materials have difficulty meeting these requirements they are modified in various ways.

Improvements in filtration efficiency and accuracy in fiber beds are provided by the use of polymeric nanofibers, i.e. fibers less than  $1\text{ }\mu\text{m}$  in diameter. A thin layer of nanofibers ( $1\text{--}5\text{ }\mu\text{m}$ ) has low strength, so it is applied over a substrate of filter materials that have greater thickness and strength, for example, cellulose, polyester or microfiber glass. An additional layer applied over standard filter materials significantly improves the efficiency and accuracy of inlet air filtration of motor vehicle engines. A great deal of research has been carried out in this area and a considerable number of studies have been written [8, 15, 17, 18, 26–28, 44, 49]. For example, the paper [8] presents the design of a new bed with a micro/nano-layered structure, and then

investigates its application in air filters. The outer layer of the composite bed is a polyester microfiber (PS) layer that has a high electrical resistance. The inner layer is polyacrylonitrile (PAN) nanofibers characterized by high polarization and small pore size. The PS/PAN/PS composite bed was examined and found to have a high filtration efficiency of 99.96% and a low pressure drop of 54 Pa for 0.30  $\mu\text{m}$  particles and at a filtration velocity of 0.053 m/s, as expressed by a quality factor of  $q_c = 0.145 \text{ Pa}^{-1}$ .

The authors of the paper [15] presented the results of testing the filtration properties of four samples made of different materials. It was shown that the filtration efficiency of the material without a layer of nanofibers for dust particles smaller than 2  $\mu\text{m}$  is very low and does not exceed 10%. It was found that a nanofiber layer (even a small one) applied to a conventional filter bed increases the filtration efficiency, the more the thickness of the layer increases. For example, for a nanofiber layer with a surface thickness of  $g_m = 0.02 \text{ g/m}^2$ , a filtration efficiency of more than 60% was obtained for particles smaller than 2  $\mu\text{m}$ . It was shown that the parameters of the filtration process: efficiency and accuracy, as well as the flow resistance of materials with an additional nanofiber layer depend on the type of substrate and the thickness of the nanofiber layer.

Similar test results with a nanofiber layer applied to a standard substrate were presented in the work [17]. A layer of nanofibers with a diameter in the range of 40–800 nm and a bed thickness of 0.3 mm and  $g_m = 0.1 \text{ g/m}^2$  was applied to a cellulose-based filter medium. The bed made in this way achieved a filtration efficiency of  $\varphi_f = 64$ –99%, with a filtration velocity of  $v_F = 0.03 \text{ m/s}$  and for dust grains in the range of  $d_p = 0.2$ –4.5  $\mu\text{m}$ . Increasing the filtration speed seven times to  $v_F = 0.2 \text{ m/s}$  resulted in a slight decrease in filtration efficiency.

The authors of the paper [18] applied a PTFE polytetrafluoroethylene membrane to a standard filter bed. The efficiency of the filter bed made in this way was determined, using nano- $\text{CaCO}_3$  powder as a test dust. The efficiency of the bed reached a value significantly higher (more than 99.99% for micron particles) compared to the standard filter material.

The paper [27] studied the effect of nanofiber content of 5%, 10%, 15%, and 20% on the filtration parameters of the cellulose bed. The proportion of 10% nanofibers in the filter bed causes a threefold increase in the flow resistance and filtration efficiency of dust grains with a size of 0.8  $\mu\text{m}$ . Regardless of the content of nanofibers in the bed, an increase in the size of dust grains within 0.03–0.2  $\mu\text{m}$  causes a decrease in filtration efficiency, and within 0.2–2  $\mu\text{m}$  its increase follows. With an increase in the compactness of nanofibers in the bed, the curve of filtration efficiency is shifted almost parallel towards larger values. The particle size at which the filtration efficiency obtained the lowest values (MPPS) on the efficiency curve was around 200 nm for all cases studied.

In [28], a submicrofiber filter medium designed to ensure the purity of engine intake air was made and tested. The filter composite was made by wet bonding two filter layers. The filtration efficiency of the composite so made was 48% and 10% higher than that of the standard bed and

the submicrofiber bed, respectively. Field tests of dust loading showed a 45% lower increase in the flow resistance of the submicrofiber bed than that of the standard bed, which was operated in a motor vehicle filter for 10,000 km.

The purpose of the study presented in [26] was to determine the effect of pore size and fiber diameter in a fiber bed and on filtration performance. One polyester bed was subjected to the study of depth filtration phenomena, and surface filtration phenomena were studied on two polyester beds covered with a polytetrafluoroethylene membrane. It was confirmed that the smaller the pore size in the bed, the higher the filtration efficiency and the higher the flow resistance.

The paper [44] presents a study of a two-stage filter constructed of two filter beds (pre-material and main material) placed at a short distance from each other. A synthetic (polypropylene) pleated filter material with low filtration efficiency and accuracy was used as the pre-filter, which was determined by large diameter fibers and high air permeability – 3100 l/(m<sup>2</sup>/s). The task of the pre-filter was to remove large dust grains. For the second filtration stage (main material), a PTFE membrane filter material applied to a cellulose substrate was used. Unlike the pre-filter, the main filter is structured with nano-sized fibers and has low permeability. The purpose of the main filter is to remove small-sized particles. This structure of the two-stage filter made it possible to significantly reduce the intensity of the increase in the flow resistance of the main filter, which increased in the correct operating time of the entire filter set, the criterion of which was the achievement of the established permissible value of flow resistance. These findings are consistent with the results of research presented in the work [10].

The authors of the paper [49] performed tests that determined the possibility of separating particulate matter from air using three tubular PTFE membrane filters that varied in diameter and length. The tests were carried out at filtration velocities in the wide range of 0.003–0.15 m/s and with particles of 10–300 nm. Efficiency curves for PTFE membranes showed a typical "V" shape for the particles used and at fixed filtration speeds. Membranes with smaller pore diameters and at flow rates with higher filtration velocities had the lowest MPPS point. It was found that two layers of membranes achieved the lowest pressure drops. Very high filtration efficiency was obtained at 99.98% for 0.3  $\mu\text{m}$  particles and almost 100% efficiency for 2.5  $\mu\text{m}$  particles.

From the above analysis it follows:

- fibrous filter beds of a layered nature show higher filtration efficiency, accuracy and mass dust loading than single layers of which a multilayer bed is made
- multilayer beds, the results of which are available in the literature, cannot be used for engine intake air filtration due to specific operating conditions, including dust concentration in the air and dust particle size. It is necessary to test filter beds that take these conditions into account
- manufacturers of filter materials for motor vehicle air filters provide for the filter manufacturer mainly their structure data such as bed thickness, pore size, grammage, air permeability. Data on filtration efficiency and accuracy, flow resistance and mass loading of dust are

not encountered. Filtration parameters can be determined, but only during experimental testing of the material with the appropriate dust and under established filtration conditions.

The purpose of this study was to evaluate the possibility of increasing engine inlet air filtration efficiency and accuracy, as well as dust absorbency, through the use of multi-layer deposits. Obtaining more favorable filtration performance in terms of filtration efficiency and accuracy will increase the life of the engine, and the higher dust absorption capacity of the bed will result in a longer life of the air filter until the permissible resistance is reached.

This is mainly due to their higher dust absorption capacity than single layers. However, it is important whether the filtration efficiency and accuracy of such a bed will obtain the appropriate and required values throughout the filter's service life. This information is not obtainable in the available literature and therefore must be obtained during experimental tests of a given material with test dust on a special stand. For this purpose, two pleated composite filter beds consisting of three standard filter materials with different properties were designed: composite K1 (polyester-glass microfiber-cellulose) and composite K2 (cellulose-glass microfiber-cellulose). In the available literature, one does not encounter studies of multilayer deposits for engine intake air filtration, which were made at the pleating stage. The constituent layers are filtration factory materials with known structure parameters. During the research, original methodology was used, which allows to obtaining of unique parameters of the filtration process of fibrous deposits, such as: initial efficiency, size of maximum grains in the air behind the filter depending on the current unit absorption of dust. The methodology allows ongoing measurement and control of changes in flow resistance as the mass of dust retained by the filter increases. These parameters are essential in the design of air filters used in automotive technology and can be used to predict vehicle mileage. Although such studies are costly and labor-intensive, this is the only way to obtain the most reliable data.

### 3. Materials and methods

#### 3.1. Subject of the study

In this study, the properties of several types of filter materials were tested, the surface of which was shaped into triangular pleats of 12 mm in height, and then cylindrical filter cartridges of the same design and dimensions and with the same area of filter material  $A_c = 0.183 \text{ m}^2$  were made from them. The cylindrical filter cartridges differed in the filter material used. The filter cartridges before testing are shown in Fig. 1.

Table 1 shows the characteristic parameters and selected properties of the filter materials to be tested. The subject of the study will be three types of filter beds. For ease of analysis of the test results, the name "Filter" is adopted and conventionally designated C, M, P, K1, K2, WP, WB.

- filter materials: C – cellulose, M – microglass, P – polyester
- composite beds K1 and K2 composed at the pleating stage of three filter layers: bed K1 (layers: P+M+C), bed K2 (layers: C+M+C) – Fig. 2–5

- filter materials: WP – non-woven polyester fabric, WB – non-woven cotton fabric.



Fig. 1. Filter cartridges prepared for testing

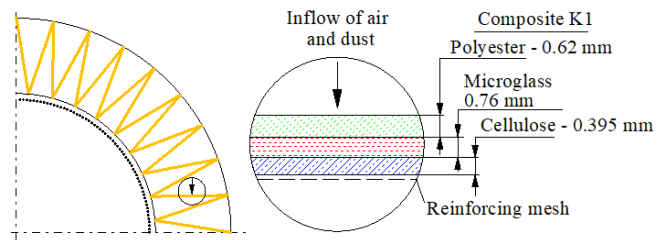


Fig. 2. Arrangement of filter layers in filter bed (composite) K1 (polyester-microglass-cellulose)

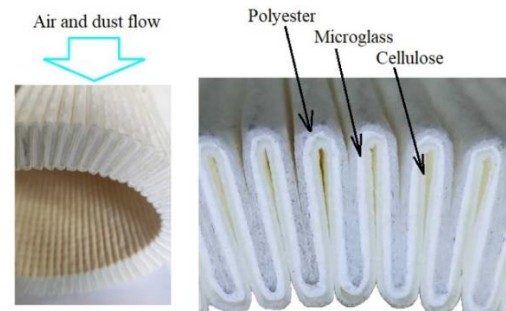


Fig. 3. Design of the K-composite (polyester-microglass-cellulose) filter: a) view of the bed after pleating, b) filter layers in the filter bed

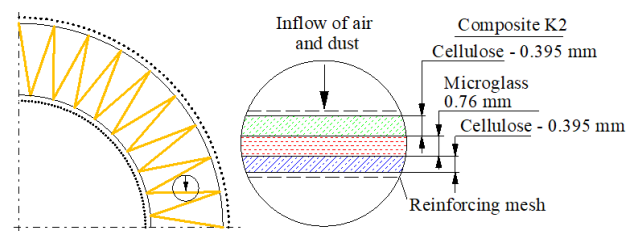


Fig. 4. Arrangement of filter layers in K2 (cellulose-microglass-cellulose) filter bed (composite)

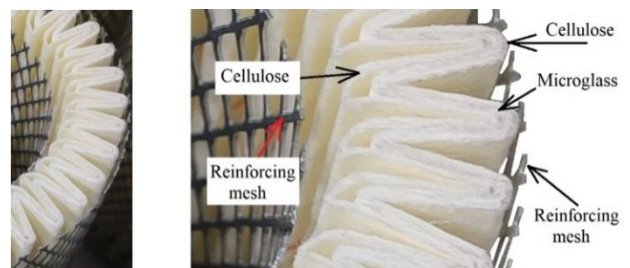


Fig. 5. K2 filter bed (composite: cellulose-microglass-cellulose) after making the pleats

Table 1. Tested filtration materials parameters according to the manufacturer's data

Filter paper identification	Material characteristics	Permeability $q_p$ [dm <sup>3</sup> /m <sup>2</sup> /s]	Grammage $g_m$ [g/m <sup>2</sup> ]	Thickness $g_z$ [mm]	Max. pore size $d_p$ [μm]
C	Cellulose	255	130	0.395	55
M	Microglass Double layer microglass media is laminated with sponbond scrim on downstream side: microglass layer 1 microglass layer 2 polyester sponbond	190	129	0.76	–
P	Polyester High hydrophobic High tensile strengths for longer pulse jet cycles	136	260	0.54	–
K1 (P-M-C)	Polyester-Microglass-Cellulose	–	–	1.775	–
K2 (C-M-C)	Cellulose-Microglass-Cellulose	–	–	1.55	–
WP	Non-woven polyester	540	442	2.5	–
WB	Non-woven cotton	–	–	–	–

### 3.2. Materials and research methods

The purpose of this study was to determine and analyze the comparative filtration properties: filtration efficiency, filtration accuracy and flow resistance of research filters made of different filtration materials: C – cellulose, M – glass microfiber, P – polyester K1 and K2 composite beds composed at the pleating stage of three filter layers (K1 bed – P-M-C layers, K2 bed – C-M-C layers), WP (non-woven polyester), WB (non-woven cotton) filter fabrics, by determining the basic characteristics as a function of mass dust load –  $k_d$ :

- particle filtration accuracy  $d_{pmax} = f(k_d)$
- particle filtration efficiency  $\varphi_f = f(k_d)$
- resistance to flow through the filter material  $\Delta p_f = f(k_d)$  and characteristics  $\Delta p_f = f(Q_f)$ , where:  $Q_f$  – the air flow rate through the active surface of the filter under test.

The mass loading of dust  $k_d$  was defined by the relation:

$$k_d = \frac{m_z}{A_c} \text{ [g/m}^2\text{]} \quad (1)$$

where:  $m_z$  – the mass of dust retained on 1 m<sup>2</sup> of the surface of the filter material, assuming its uniform distribution over the entire surface,  $A_c$  – the area of the active surface of the filter paper of the tested filter – the area of the filter paper through which the air stream flows.

The filtration velocity is the quotient of the air stream flowing through the filter  $Q_{fmax}$  and the area of the active surface  $A_c$ :

$$v_F = \frac{Q_f}{A_c \times 3600} \text{ [m/s]} \quad (2)$$

Filter tests were performed on a bench (Fig. 6) equipped with the necessary equipment and instruments for recording the data necessary for determining filter characteristics. A  $P_{amas}$  particle counter was used to record the size and number of particles in the  $Q_f$  stream downstream of the filter under test, allowing measurement in  $i = 32$  measurement intervals in the range of 0.7–100 μm. The polluted air stream was drawn to the counter's sensor from the measuring line behind the filter under test, where the tip of the measuring probe was centrally located. The measuring line was terminated with a special filter, which protects the flow meter sensor from dust, and at the same time is a measuring (absolute) filter used to determine the filtration efficiency. To measure the air flow rate  $Q_f$ , an FMT430 mass flow

meter was used, which has a measuring range of 10–150 m<sup>3</sup>/h and an accuracy of 1.2%.

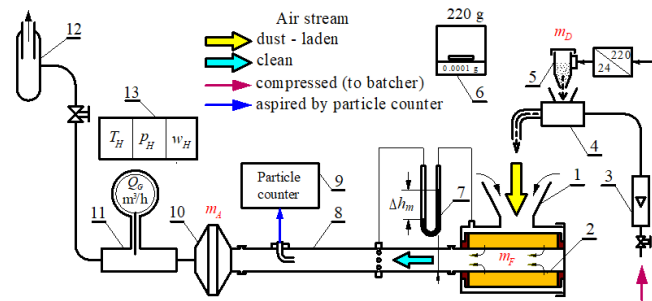


Fig. 6. Schematic of a standard test stand for testing air filters of internal combustion engines of vehicles with air demand up to 350 m<sup>3</sup>/h: 1 – dust chamber, 2 – filter cartridge, 3 – rotameter, 4 – dust dispenser, 5 – dust tank, 6 – analytical balance, 7 – U-tube pressure gauge, 8 – measuring tube, 9 – counting device, 10 – measuring (safety) filter, 11 – mass air flow meter, 12 – fan forcing the flow, 13 – instrument for measuring humidity, temperature and ambient pressure

An electromagnetic metering device with an oscillating dust hopper and pneumatic (compressed air) transport of dust to the dust chamber, where it is mixed with the air inlet stream and flows into the filter, was used to supply dust to the test filter. PTC-D test dust was used, which is a substitute for AC fine test dust in Poland [11]. The main components of this dust and its fractional composition are exposed in Fig. 7. The dust contains more than 67% quartz (SiO<sub>2</sub>) grains, a mineral characterized by high hardness, causing accelerated wear of engine components.

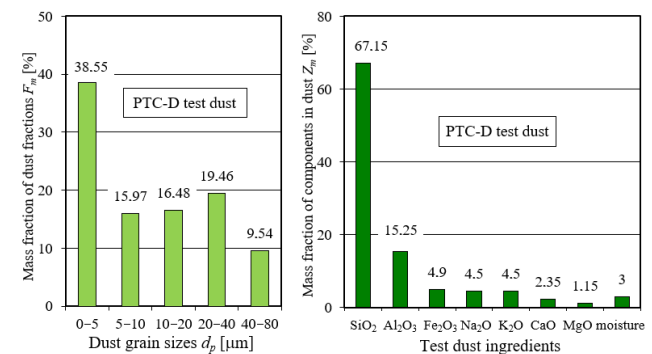


Fig. 7. Characteristics of PTC-D test dust: (a) factual composition of dust, (b) chemical composition of dust. The figure is based on data in [11]

The flow characteristics  $\Delta p_f = f(Q_f)$  of filters C, M, P, K1, K2, WP, and WB were determined at 10 measurement points as a function of air flux varying within the limits  $Q_f = Q_{fmin} - Q_{fmax}$ .

The maximum value of the flux  $Q_{fmax}$  was determined from relation (3) assuming the maximum filtration velocity  $v_F = 0.1$  m/s. According to the authors of works [3, 12, 46], for proper operation of passenger car air filters, the maximum filtration velocity should be within the limits  $v_F = 0.06 - 0.12$  m/s.

$$Q_{fmax} = A_c \cdot v_F \cdot 3600 \text{ [m}^3/\text{h]} \quad (3)$$

Characterizations of the filters: efficiency  $\varphi_f = f(k_d)$  and filtration accuracy  $d_{pmax} = f(k_d)$ , as well as flow resistance  $\Delta p_f = f(k_d)$  were performed simultaneously according to the same methodology on the bench (Fig. 6) for one fixed value of air flow  $Q_j = 56$  m<sup>3</sup>/h, which corresponds to the speed of flow through the filter material  $v_F = 0.085$  m/s. A measurement cycle was established, the duration of which was equivalent to the time of uniform dust dosing at a fixed air flow rate  $Q_j$ . The filtration efficiency  $\varphi_f = f(k_d)$  was determined by the gravimetric method (measurement of the weight of the filter, the dispenser and the absolute filter before and after the measurement cycle) for a constant air flow and successively repeated  $j$  test cycles of fixed duration  $\tau_{pd}$ . The measurement time (duration of one cycle) was fixed:  $\tau_{pd} = 2$  min. in the initial period and  $\tau_{pd} = 4 - 5$  min. in the main period of filter operation. The mass loss of dust from the dispenser  $m_D$  (the mass of dust delivered to the filter) and the mass of dust retained on the tested filter  $m_F$  and the absolute filter  $m_A$  were determined with an analytical balance with a measuring range of 220 g and an accuracy of 0.1 mg. Switching on the particle counter to measure the number and size of dust grains in the air stream behind the filter was set 60 seconds before the scheduled end of the measurement cycle. During one measurement cycle, three particle counts were programmed at the planned measurement intervals ( $d_{pimin} - d_{pimax}$ ), and their average value was used for analysis.

After the measurement cycle  $j$ , the parameters of the filtration process were recorded to calculate filtration efficiency, filtration accuracy, flow resistance and mass loading of dust  $k_d$ .

1. The efficiency of the filter was calculated as the quotient of the mass of dust  $m_{Fj}$  retained and the mass of dust  $m_{Dj}$  delivered to the filter during the next  $j$  measurement cycle, from the relation:

$$\varphi_j = \frac{m_{Fj}}{m_{Dj}} = \frac{m_{Fj}}{m_{Fj} + m_{Aj}} 100\% \quad (4)$$

2. The mass loading of dust  $k_{dj}$  of the filter material used in the filter was calculated from the relationship:

$$k_{dj} = \frac{\sum_{j=1}^n m_{Fj}}{A_c} \text{ [g/m}^2\text{]} \quad (5)$$

3. The number  $N_{pi}$  of dust grains in the air stream  $Q_f$  downstream of the filter in fixed and diameter-limited ( $d_{pimin} - d_{pimax}$ ) measurement intervals from the particle counter printout.

4. Filtration accuracy as the largest dust grain size  $d_{pj} = d_{pmax}$  occurring in the air stream  $Q_f$  downstream of the filter and appearing on the particle counter printout.
5. The proportion of the measured  $N_{pi}$  number of dust grains in each measurement interval relative to the total number of dust grains passed through the filter for a given test cycle:

$$U_{pi} = \frac{N_{pi}}{N_p} = \frac{N_{pi}}{\sum_{i=1}^{32} N_{pi}} 100\% \quad (6)$$

where:  $N_p = \sum_{i=1}^{32} N_{pi}$  – the total (from all measurement intervals) number of dust grains present in the airstream downstream of  $Q_f$  after the test filter.

6. Flow resistance  $\Delta p_{fj}$  of the filter being the difference in static pressure upstream and downstream of the filter calculated according to the following relationship:

$$\Delta p_{fj} = \frac{\Delta h_{mj}}{1000} \cdot (\rho_m - \rho_H) \cdot g \text{ [Pa]} \quad (7)$$

where:  $\Delta h_{mj}$  – height measured on a U-tube water pressure gauge after dust dosing,  $\rho_m$  – density of the manometric liquid [kg/m<sup>3</sup>],  $\rho_H$  – density of air [kg/m<sup>3</sup>],  $g$  – earth's attraction [m/s<sup>2</sup>].

According to the above methodology, the characteristics of efficiency  $\varphi_f$  and filtration accuracy  $d_{pmax}$  and flow resistance  $f(k_d)$  of filters C, M, P, K1, K2, WP, WB were determined depending on the mass of dust retained on the filter and defined as "mass loading of dust"  $k_d$  [g/m<sup>2</sup>]. Two copies of each filter were tested with the same filter material and under the same conditions. Before testing the filters with dust, their  $\Delta p_f = f(Q_f)$  characteristics were performed.

#### 4. Research results and their analysis

Figure 8 shows the changes in flow resistance  $\Delta p_f$  of the tested filters with different filter materials as a function of the air flow rate  $Q_f$ . Regardless of the filter tested, the increase in air flow rate causes a parabolic increase in flow resistance  $\Delta p_f$ , which is due to the increase in flow velocity through the bed in the second power.

The highest values of flow resistance, over the entire range of air flow  $Q_f$ , were recorded for the cartridge, where the filter bed is a K2 composite (C + M + C) of three sequentially arranged layers: cellulose, microglass and cellulose. For  $Q_{fmax} = 56$  m<sup>3</sup>/h, the flow resistance of the K2 cartridge has a value of  $\Delta p_f = 1.304$  kPa (Fig. 8). This value is more than 2.5 times higher than the flow resistance value of material C, which is exclusively a cellulose filter material. Similarly high flow resistance is characterized by composite K1 (P + M + C) of three sequentially arranged layers: polyester, microglass and cellulose. Such significant values of flow resistance are mainly due to the thickness of the composite deposits, which are the sum of the thickness of the three layers of filter material folded together. Composite K2 has a thickness of  $g_z = 1.55$  mm, and K1  $g_z = 1.775$  mm. In comparison, the thickness of the cellulose layer is  $g_z = 0.395$  mm. The flow resistance of the other filters is at a much lower level in the range  $\Delta p_f = 0.471 - 0.696$  kPa for a flow rate of  $Q_f = 56$  m<sup>3</sup>/h.

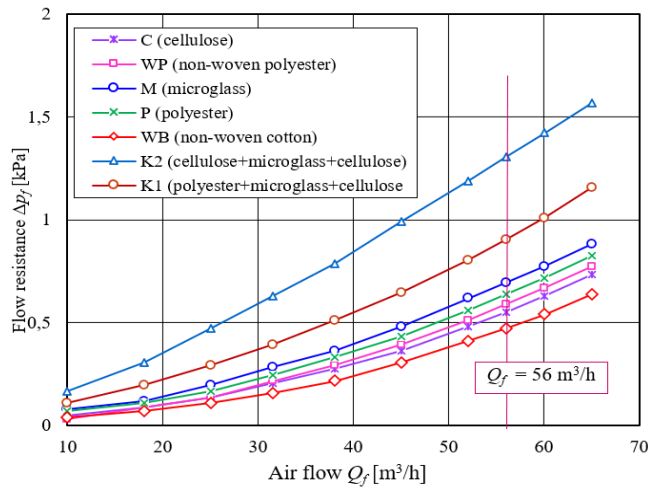


Fig. 8. Flow resistance characteristics  $\Delta p_f = f(Q_f)$  of filters with different filter materials

The filtration characteristics: efficiency  $\varphi_f = f(k_d)$  and filtration accuracy  $d_{pmax} = f(k_d)$  and flow resistance  $\Delta p_f = f(k_d)$  of the filter materials C, M, P, WP, WB and composites K1 and K2 made by the author for the study are shown in Fig. 9–19. The characteristics are similar as to the course, but differ as to the obtained values of efficiency, filtration accuracy and flow resistance depending on which filter material they are made of. At the onset of the filtration process, filtration efficiency and flow resistance take on small but varying values, which with the increase in the dust mass on the filter layer (increase in the mass loading of dust  $k_d$ ) take on increasing values, which is characteristic of fibrous deposits. The increase in filter performance values is due to changes in the structure of the filter bed, which result from the retention of dust grains on the fibers of the filter bed through the action of filtration mechanisms, mainly: inertial, direct retention and diffusion. The first dust particles retained and deposited on the surface of the fibers form a layer on which further dust grains arriving with the air are deposited. Successive layers of dust are superimposed, which form agglomerates that often grow to considerable sizes. In this way, the free spaces between the fibers are filled. The phenomenon of the formation of dust agglomerates on fibers is discussed in detail in the paper [23].

Agglomerates formed on the fibers cause a change in the conditions of air flow and separation of successive dust grains. The distances between the surfaces of dust-laden elements decrease (the porosity of the baffle decreases), which causes an increase in flow velocity, and hence the hydrodynamic flow resistance in the filtration layer must increase as a consequence. Reducing the distance between the dust-laden fibers increases the intensity of the filtration mechanisms, hence the filtration efficiency obtains higher and higher values and gets closer and closer to 100%. From this point on, the filtration efficiency usually remains constant. Therefore, the filtration process of the studied filters was conventionally divided into two stages. It was determined that the first ( $t_{p1}$ ), the initial stage of each filter's operation, lasts from the beginning of the influx of dust onto the filter until the filtration efficiency reaches  $\varphi_f = 99.9\%$ . This efficiency value is required of filter materials

intended for motor vehicle engine intake air filters. The following stage of operation is called the main stage and lasts until the filter reaches the set value of flow resistance.

The filtration accuracy, defined as the maximum size of dust grains behind the filter, initially has a small value. In the air behind the filter there are initially dust grains  $d_{pmax}$  of large size, after which they decrease with the increase of the mass loading of dust  $k_d$  and remain constant for a while, then at the end of the filtration process they generally reach larger and larger values, which is generally associated with a decrease in efficiency and means that the filtering capacity of the filter is exhausted. The direct cause of the appearance of large dust grains in the air behind the filter at the final stage of filtration is the large flow resistance, the value of which increased intensively with the increase in the mass loading of dust  $k_d$  of the filter bed. With a large pressure difference and high local flow velocities in the filter bed, dust grains are detached, from the outermost parts of the agglomerates, and migrate towards the outlet. It follows from the above that the operation of the air filter with excessive flow resistance is inadvisable. Therefore, it was assumed that the criterion for completing the testing of filters would be the achievement of a fixed value of resistance, called in the literature the permissible resistance  $\Delta p_{fidop}$ . In the case of the tested filters, the value  $\Delta p_{fidop} = 4$  kPa was assumed.

Figures 9–11 show the characteristics of filtration efficiency  $\varphi_f = f(k_d)$ , filtration accuracy  $d_{pmax} = f(k_d)$  and flow resistance  $\Delta p_f = f(k_d)$  of filters with a filtration bed, respectively: C (cellulose), M (microglass) and P (polyester).

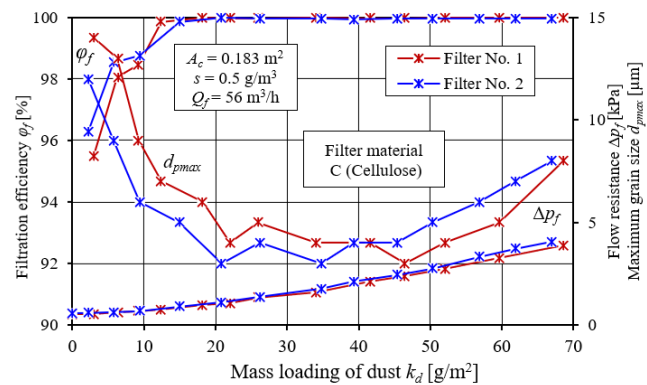


Fig. 9. Changes in efficiency  $\varphi_f$  and filtration accuracy  $d_{pmax}$ , as well as flow resistance  $\Delta p_f$  as a function mass loading of dust  $k_d$  of the tested filters with filter bed C (cellulose)

Two filters were tested for each filter material. You can notice slight differences in the characteristics and in the obtained values of efficiency, filtration accuracy and flow resistance for two filters made of the same type of filter material.

A comparative analysis in terms of changes in filtration efficiency and accuracy, as well as flow resistance as a function of the mass loading of dust  $k_d$  of C, M and P filter beds is shown in Fig. 12.

The characteristics of No. 2 filters of each type of filter material were used. The characteristic curves vary, which is mainly due to the structure of the materials studied.

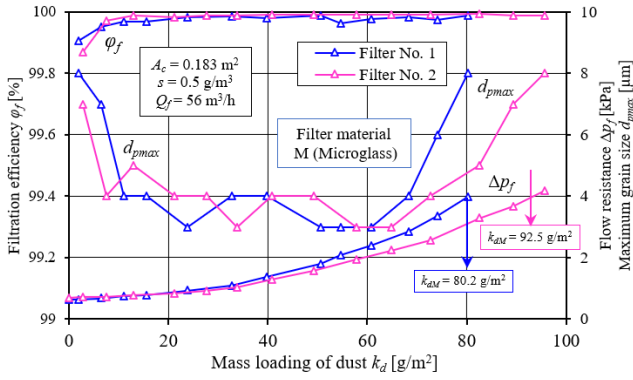


Fig. 10. Changes in efficiency  $\phi_f$  and filtration accuracy  $d_{pmax}$ , as well as flow resistance  $\Delta p_f$  as a function mass loading of dust  $k_d$  of the tested filters with filter bed M (microglass)

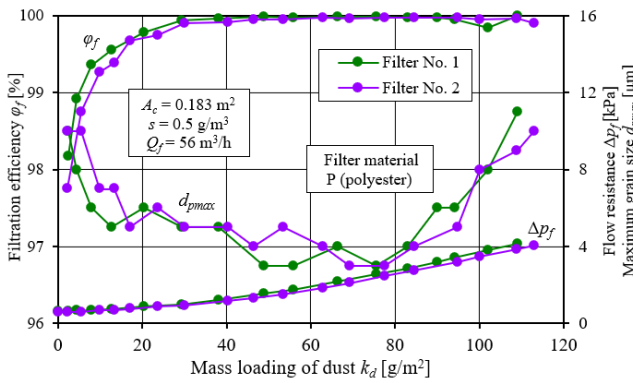


Fig. 11. Changes in efficiency  $\phi_f$  and filtration accuracy  $d_{pmax}$ , as well as flow resistance  $\Delta p_f$  as a function mass loading of dust  $k_d$  of the tested filters with material P (polyester)

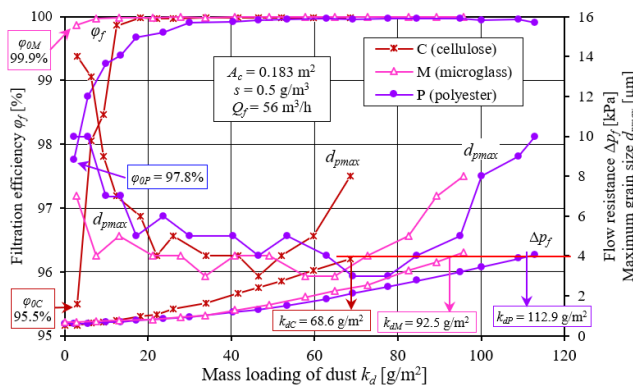


Fig. 12. Comparative analysis of filtration properties in terms of filtration efficiency and accuracy, flow resistance and mass loading of dust of bed filters: C, M and P

Material C, which obtained the lowest ( $\phi_{0C} = 95.5\%$ ) filtration efficiency during the initial period, has at the same time the highest permeability ( $q_p = 255 dm^3/m^2/s$ ) and the smallest ( $g_m = 130 g/m^2$ ) grammage (Table 1), which means that mainly depth filtration takes place in the bed, which does not guarantee high efficiency of dust grain retention. Material M (microglass), which has a much lower permeability ( $q_p = 190 dm^3/m^2/s$ ) and a comparable grammage, achieved a very high initial filtration efficiency ( $\phi_{0M} = 99.9\%$ ). This is due to the fact, this material is constructed of two layers of very thin glass fibers and protected at the

outlet by a layer of polyester (Table 1). This guarantees the occurrence of the phenomenon of surface filtration and the retention of dust grains of small size and ensures a high ( $k_{dM} = 92.5 g/m^2$ ) mass loading of dust (Fig. 12).

Figures 13 and 14 show the characteristics of filtration efficiency  $\phi_f = f(k_d)$ , filtration accuracy  $d_{pmax} = f(k_d)$  and flow resistance  $\Delta p_f = f(k_d)$  of filters with filter bed, respectively: WP (non-woven polyester), WB (non-woven cotton). It can be seen the high reproducibility of the obtained test results for both WB and WP nonwovens.

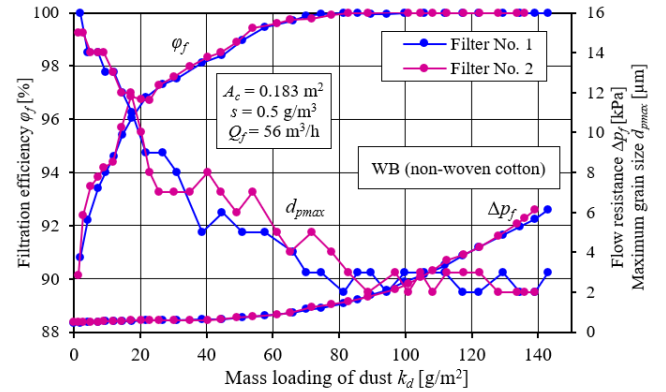


Fig. 13. Changes in efficiency  $\phi_f$  and filtration accuracy  $d_{pmax}$ , as well as flow resistance  $\Delta p_f$  as a function mass loading of dust  $k_d$  of the tested filters with WB material (non-woven cotton)

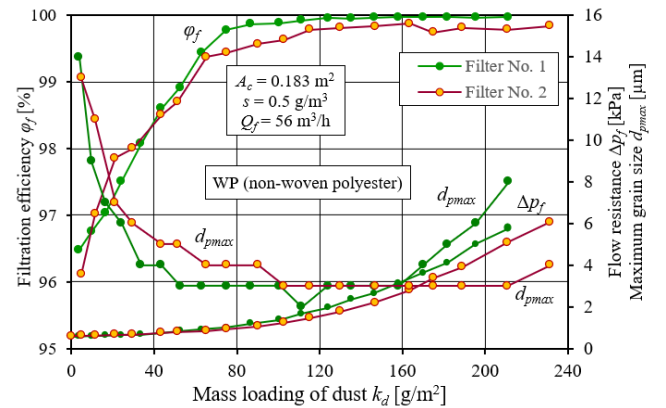


Fig. 14. Changes in efficiency  $\phi_f$  and filtration accuracy  $d_{pmax}$ , as well as flow resistance  $\Delta p_f$  as a function of mass loading of dust  $k_d$  of the tested filters with WP (non-woven polyester) material

Figure 15 analyses the changes in filtration efficiency, filtration accuracy and flow resistance as a function of the dust mass loading  $k_d$  of the WB and WP filter beds. The results of tests on filter No. 2 of both nonwovens were used for the analysis. Analyzing the slow increase in filtration efficiency and accuracy as a function of dust mass load  $k_d$ , it should be noted that the duration of the initial filtration period of both nonwovens is significant. The initial filtration efficiency of the nonwovens obtains small values  $\phi_{0WB} = 90.8\%$  and  $\phi_{0WP} = 96.1\%$ , respectively. In order for the filters to achieve the required filtration efficiency of  $\phi_f = 99.5\%$ , it is necessary to achieve a mass loading of the dust of  $k_{dWB1} = 65.96 g/m^2$  and  $k_{dWP1} = 115.4 g/m^2$ , respectively, which is more than 50–70% of the total filter operation time to achieve the established permissible flow resistance  $\Delta p_{fidop}$

= 4 kPa (Fig. 15). During this time, dust grains of considerable ( $d_{pmax} = 14\text{--}16\ \mu\text{m}$ ) size were recorded in the air behind the filter. However, the grain sizes decreased as the mass of dust retained on the filter bed increased, and by the end of the initial period they had stabilized at  $d_{pmax} = 3\text{--}4\ \mu\text{m}$ . Under conditions of actual filter operation, the engine is exposed to dangerous dust. An apparent increase in the flow resistance of the tested filters began when the initial period ended and the main period of filter operation began, during which the filtration efficiency remained high, more than 99.5%. The significant increase in flow resistance was due to the higher intensity of dust accumulation in the bed as a result of the high efficiency. A filter material with such properties cannot be suitable for filtering engine intake air but can be used as a pre-filter in a two-stage filtration system.

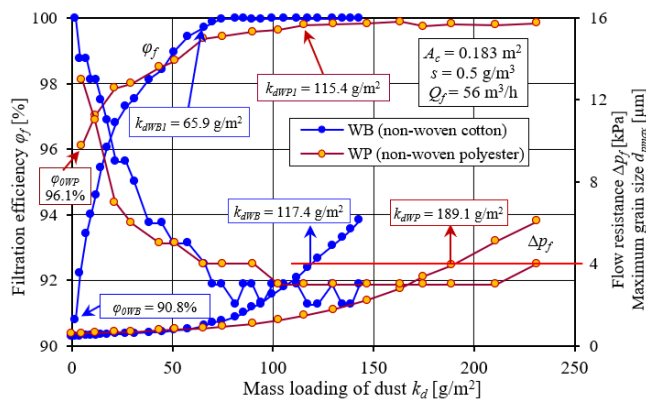


Fig. 15. Comparative analysis of filtration properties in terms of filtration efficiency and accuracy, flow resistance and mass loading of dust of filters with WP (non-woven polyester) and WB (non-woven cotton) material

The characteristics of filtration efficiency  $\phi_f = f(k_d)$ , filtration accuracy  $d_{pmax} = f(k_d)$  and flow resistance  $\Delta p_f = f(k_d)$  of two copies of K1 (P-M-C) composite filter bed filters, presented in Fig. 16, show great similarity as to their course and values. The tested filters achieve a high initial filtration efficiency of  $\phi_{0K1} = 99.87\%$  (for  $k_{dKp} = 5.95\ \text{g/m}^2$ ), and the size of maximum dust grains during the initial period does not exceed the value of  $d_{pmax} = 5\text{--}7\ \mu\text{m}$ . After the cartridges reach a mass loading of dust of  $k_{dK1} = 16.3\ \text{g/m}^2$ , the sizes of maximum dust grains stabilize at  $d_{pmax} = 2\text{--}3\ \mu\text{m}$ , which is a very high accuracy for fibrous filter media that can be used in automotive technology. The high filtration efficiency and accuracy of the cartridges was maintained until the flow resistance  $\Delta p_f = 6.2\ \text{kPa}$  was reached (Fig. 16). The filter elements tested achieved a high mass loading of dust of  $k_{dK1} = 199.8\ \text{g/m}^2$ , which is due to the configuration of the materials used and the considerable ( $g_m = 1.775\ \text{mm}$ ) thickness of the composite bed. The first filter layer of the K1 cartridge is a 0.62-mm-thick polyester bed with high permeability, which makes the phenomenon of depth filtration occur, resulting in the retention of dust grains of the largest size. The second filtration layer is M bed (microfiber glass), where the phenomenon of surface filtration occurs, resulting in high efficiency and accuracy of filtration of small-sized dust grains (Fig. 12). The cellulose layer is a reinforcing layer and stabilizes the airflow.

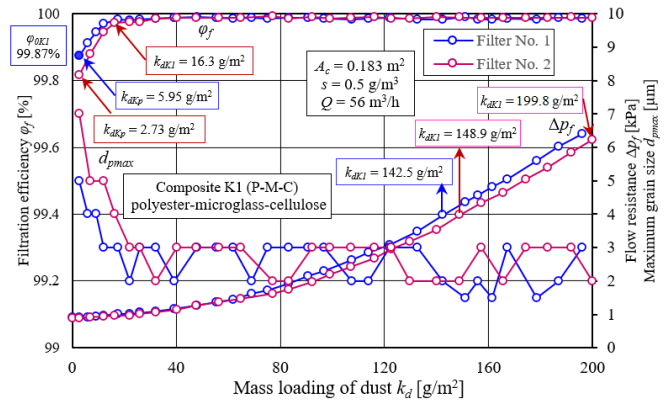


Fig. 16. Variation of efficiency  $\phi_f$  and filtration accuracy  $d_{pmax}$  and flow resistance  $\Delta p_f$  as a function mass loading of dust  $k_{dK1}$  of K1 filter with composite bed of three layers: P-M-C

On the other hand, Fig. 17 shows a comparative analysis of the filtration properties of composite K1 (P-M-C) and composite K2 (C-M-C), whose filtration characteristics were performed under the same assumed conditions. It can be clearly seen that the K1 composite, which differs only in the first filtration layer (polyester) from the K2 composite (cellulose), achieves significantly better results in terms of filtration efficiency and accuracy.

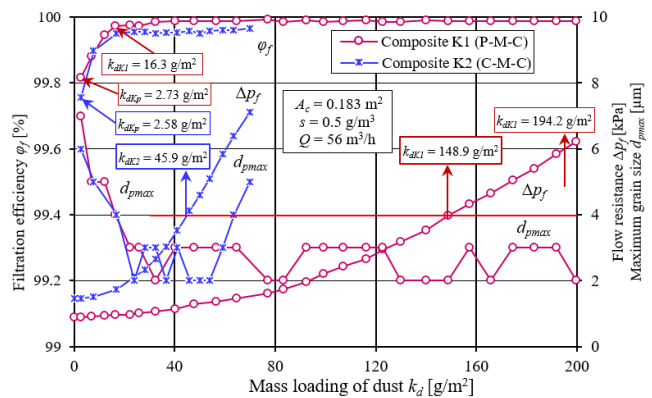


Fig. 17. Characteristics of filtration efficiency  $\phi_f = f(k_d)$ , filtration accuracy  $d_{pmax} = f(k_d)$  and flow resistance  $\Delta p_f = f(k_d)$  of filters with composites: K1 (P-M-C) and K2 (C-M-C)

After the K1 composite reaches a mass loading of dust  $k_{mK1} = 16.3\ \text{g/m}^2$ , the filtration efficiency is at 99.99% and is maintained until the flow resistance  $\Delta p_f = 6.2\ \text{kPa}$  is reached, which is well beyond the permissible resistance (Fig. 17). It should be noted that at this time there are dust grains of very small size  $d_{pmax} = 3\text{--}4\ \mu\text{m}$  in the exhaust air from the tested filter.

When the flow resistance  $\Delta p_{fdop} = 4\ \text{kPa}$  is reached, the mass loading of dust of the K1 composite is  $k_{dK1} = 148.9\ \text{g/m}^2$ , which is three times higher than that of the K2 composite, for which  $k_{dK2} = 45.9\ \text{g/m}^2$ . This is due to the increase in flow resistance of the tested materials K1 and K2. As can be seen from Fig. 17, the intensity of the increase in flow resistance of K2 is very high, which may be due to the low efficiency of the C (cellulose) layer and the deposition of most of the dust on the M (fiberglass) filter bed.

From the research presented here, it can be seen that there is a close relationship between the filtration efficiency and flow resistance and the filtration accuracy of the filter material. An increase in filtration efficiency is directly related to an increase in filter accuracy ( $d_{pmax}$  decreases) and an increase in flow resistance. Comparing directly the filtration properties of different materials is difficult. Therefore, the “filtration quality factor  $q_c$ ” is commonly used in the literature, which relates filtration efficiency and flow resistance of the same filter material and, according to [32, 46], is expressed by the relation:

$$q_c = \frac{-\ln(1-\varphi_{f0})}{\Delta p_f} [1/kPa] \quad (8)$$

where:  $\varphi_{f0}$  – initial filtration efficiency,  $\Delta p_f$  – flow resistance.

A higher value of  $q_c$  means a more favorable relationship between efficiency and flow resistance, which means that the filtration process is more efficient.

In addition, for the purpose of this work, to compare the filtration properties of the tested materials, the filtration efficiency index  $q_s$ , was defined, which expresses in (%) the period of correct operation of the filter concerning the total time of its operation:

$$q_s = \left(1 - \frac{k_{d1}}{k_{d2}}\right) 100\% \quad (9)$$

where:  $k_{d1}$  – mass loading of dust of the material at the time of obtaining the required filtration efficiency  $\varphi_f = 99.5\%$ ,  $k_{d2}$  – mass loading of dust of the material at the time of obtaining by the filter the established permissible resistance ( $\Delta p_{fidop} = 4$  kPa).

A smaller value of the  $q_s$  index means a shorter duration of the filtration process with the required filtration efficiency and accuracy.

Using the above relationships, the values of  $q_c$  and  $q_s$  coefficients were calculated for the tested filter materials, and the results are summarized in Fig. 18.

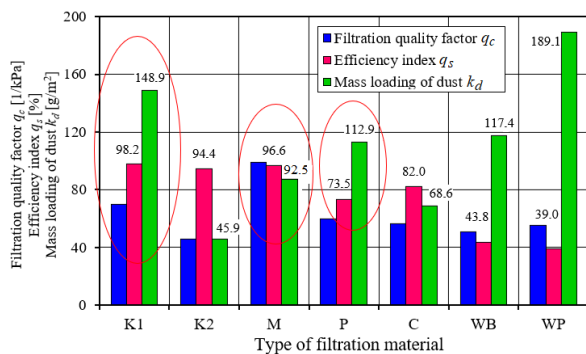


Fig. 18. Filtration quality factor  $q_c$ , efficiency index  $q_s$ , and mass loading of dust  $k_d$  of the tested filter materials

## 5. Vehicle mileage modeling

Determining the duration of proper operation of an air filter is not a straightforward exercise since it depends on many factors that change during vehicle use. The operating time of a filter can be determined experimentally during its use in a vehicle or during tests on a laboratory bench. Depending on the type and size of the air filter, such tests are usually labor-intensive and expensive. The basic criterion

for completing the tests is the achievement of a fixed value of the permissible flow resistance  $\Delta p_{fidop}$ . It is also possible to computationally determine the operating time  $\tau_{pf}$  of an air filter using theoretical relationships, such as that given in [29]:

$$\tau_{pf} = \frac{A_c \cdot k_d \cdot k_c}{Q_{E_{max}} \cdot s \cdot \varphi_f} [h] \quad (10)$$

where:  $A_c$  – active surface area of the filter material in the filter [m<sup>2</sup>],  $k_d$  – mass loading of dust of the filter material [g/m<sup>2</sup>] at the permissible value of the flow resistance  $\Delta p_{fidop}$ ,  $k_c$  – correction factor for the difference between the test dust parameters and the parameters of the real pollution,  $Q_{E_{max}}$  – nominal engine inlet air flow [m<sup>3</sup>/h],  $s$  – dust concentration in the air entering the filter [g/m<sup>3</sup>],  $\varphi_f$  – filtration efficiency of the filter material.

If we assume a constant (average) driving speed  $V_p$  (km/h), the distance traveled by the vehicle  $S_p$  in time  $\tau_{pf}$  is described by the formula:

$$S_p = \tau_{pf} \cdot V_p [km] \quad (11)$$

If we now consider relation (9), then the distance the vehicle will travel in time  $\tau_{pf}$  can be described by the relation:

$$S_p = V_p \frac{A_c \cdot k_d \cdot k_c}{Q_{E_{max}} \cdot s \cdot \varphi_f} [km] \quad (12)$$

From the presented relationship, it is clear that for its practical application it is necessary to know several data that describe the filter material, which are: filtration efficiency  $\varphi_f$ , mass loading of dust  $k_d$ , and coefficient  $k_c$ , which corrects the difference between test and actual parameters under specific operating conditions. Among the most important are the chemical composition of the dust, the type of dust and its concentration, the granularity of the dust, and the speed of the airflow. The  $k_c$  factor is mainly used when the effect of soot on the operating time of a pleated paper cartridge filter must be considered. The  $k_c$  factor is usually defined as the ratio of the filter operating time under soot contamination conditions to the operating time when using test dust, which is mineral dust. With higher soot content in the air, the  $k_c$  factor takes values less than 1, and the filter's operating time will be correspondingly shorter. This is important in the case of passenger car air filters operated in urban conditions, where soot, as a product of incomplete combustion of fuel in engines, is the predominant pollutant of the air entering the engine, but also of the air inhaled by people.

Filter materials are produced by specialized plants, which describe their structure with characteristic parameters, this is most often: material thickness and grammage, pore dimensions and air permeability at specific flow parameters. Manufacturers also specify the type of filter material or the percentage composition of the component. As can be seen, none of these data is a component of the relationship (11). Previous studies of modern fibrous filter materials applicable in automotive technology report that their filtration efficiency oscillates within narrow limits  $\varphi_f = 99.5\text{--}99.9\%$  during the main period of filter operation. Such efficiency values were registered during the tests described in this paper.

It follows that the parameter that, in relation (11), significantly determines the course of the  $S_p$  vehicle is the mass loading of dust  $k_d$  of the filter material used. From the tests carried out in this work, it can be seen that there are significant differences in the achieved values of the mass loading of dust  $k_d$  for different filter materials determined at the permissible flow resistance, in this case for  $\Delta p_{fdop} = 4$  kPa. Using the calculated values of the  $k_d$  coefficient for cellulose C and composite K and taking the values of the other parameters in relation (11) as constants, the modeled mileages of a passenger car at which filter servicing – replacement of the filter element – should be carried out were established.

Using relation (11), calculations were carried out based on the data of the Audi A4 engine (CI engine with turbocharging and air cooler): displacement  $V_{ss} = 2.496$  dm<sup>3</sup>, filter paper area  $A_c = 2.09$  m<sup>2</sup>, engine inlet air flow  $Q_{Emax} = 554$  m<sup>3</sup>/h. For the calculations, it was assumed that the test vehicle would be used mainly in non-urban conditions, where dust is the main component of pollution. Therefore, a correction factor of  $k_c = 1$  was assumed. According to [3], the dustiness of air on paved roads and highways can take on values in the wide range of  $s = 0.0004–0.1$  g/m<sup>3</sup>. To calculate the vehicle mileage (achieving  $\Delta p_{fdop}$ ), the use of the vehicle was assumed at an air dust concentration of  $s = 0.0005$  g/m<sup>3</sup> and a vehicle moving speed of  $V_p = 60$  km/h. Vehicle mileage was estimated for a vehicle equipped with an air filter with composite K1 and materials that are successive layers in this composite: P, M and C. The dust mass load  $k_d$  and filtration efficiency  $\varphi_f$  were adopted from filter tests. The results of the calculations are shown in Fig. 19.

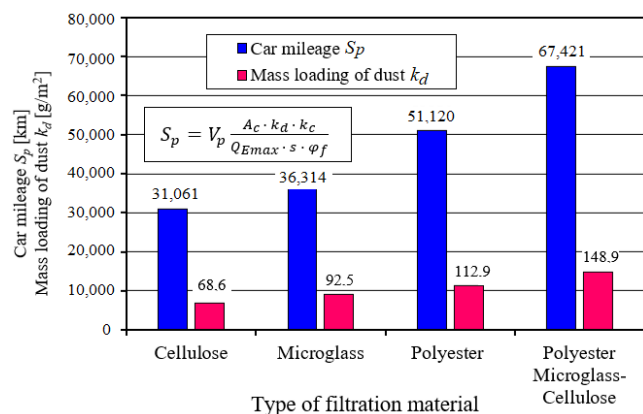


Fig. 19. Modeled car runs for different types of filter beds and corresponding different mass loading of dust  $k_d$

As expected, the higher the mass loading of dust  $k_d$ , the higher the vehicle mileage has a higher value (Fig. 19). A filter with a filter material (K-composite made by the author) provides twice the mileage of the other filter materials, which is due to the correspondingly higher mass loading of dust  $k_d$ . For the assumptions made, the modeled vehicle mileage has a value of more than 67,000 km. The mileage values are subject to change depending on changes in vehicle operating conditions, such as dust concentration in the air drawn into the engine, driving speed and air flow  $Q_E$ , which does not often assume maximum values. The mileage of the vehicle is largely determined by the filter

area of the  $A_c$  material. Due to the limited space around the engine, where the air filter is most often located, it is difficult to apply a sufficiently large filter paper surface.

Figure 20 shows that an increase in the concentration of dust in the air increases, at the same value of air flow, the mass of dust delivered to the filter which fills the filter bed with greater intensity. Since the absorptive capacity of the filter bed is limited, the value of the vehicle mileage is shortened accordingly. For filter beds whose dust load  $k_d$  the vehicle mileage will be lower. A change in dust concentration within  $s = 0.0005–0.001$  g/m<sup>3</sup> reduces the mileage of the car by 50% regardless of the absorptive capacity of the filter material  $k_d$ .

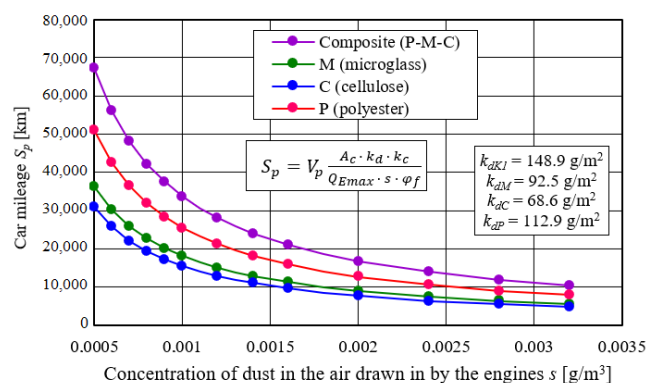


Fig. 20. Modeled car runs depending on the dust concentration in the inlet air for different mass loading of dust  $k_d$  of filter beds

## 6. Summary and final conclusions

The purpose of the study was to experimentally evaluate the properties of filter materials in the context of selecting a filter material with the best parameters for the filtration of air drawn by vehicle internal combustion engines. The evaluation was based on the filtration characteristics determined on the test bench: filtration efficiency and accuracy, as well as flow resistance depending on the mass loading of dust  $k_d$ . Filter materials produced by specialized factories were tested: cellulose, polyester, microfiber glass, and a filter bed made of three layers of different materials. A filter bed consisting of three base filter materials (polyester-microglass-cellulose) was designed and fabricated, and the characteristics of the filter bed were determined. A comparative analysis was carried out using the air filtration quality coefficients of the fiber baffles. The results of the study and their analysis led to the following conclusions.

- 1) Two characteristic stages can be distinguished in the filtration process of the tested filter beds: a preliminary stage showing a low initial, but increasing with the influx of dust on the bed, efficiency  $\varphi_f$  and filtration accuracy  $d_{pmax}$ , and a small but slowly increasing flow resistance  $\Delta p_f$ , and a main stage, which starts when a stable efficiency is reached at the conventional minimum level of  $\varphi_f = 99.5\%$ .
- 2) The duration of the pre-stage varies for the filter materials tested and is longer the lower the initial filtration efficiency. For WB and WP nonwovens, this is 96.1% and 90.8%, respectively. This increased the duration of the initial stage and reduced the main stage to 40% of the

total filter operating time with these materials. This has a major impact on the accelerated wear of the engine's tribological associations, due to the large-diameter dust grains ( $d_{pmax} = 14\text{--}16\ \mu\text{m}$ ) in the air behind the filter at this time, which are drawn into the engine cylinders.

- 3) The filter bed (K1 composite) made for the present study, in the form of three composite layers of polyester-glass microfibre-cellulose materials, shows, under the same test conditions as the other materials, a high initial filtration efficiency (99.8%) and thus a short initial filtration period. This resulted in a prolongation of the duration of the main stage involving the filtration process with high efficiency (99.9%) and filtration accuracy ( $d_{pmax} = 1.5\text{--}3\ \mu\text{m}$ ) until the set flow resistance value  $\Delta p_{fidop} = 4\ \text{kPa}$  was reached.
- 4) Compared to other tested materials, the K1 composite obtained more than twice the value of the mass dust load ( $k_{dK1} = 148.9\ \text{g/m}^2$ ), which will allow to extend the operating time of the filter (vehicle mileage in km) until the performance of air filter servicing – filter cartridge replacement.
- 5) The presented original methodology for experimental testing of filter materials having different chemical composition structure parameters, and thus different filtration properties, partly fills the information gap in the acquisition of basic parameters of filter materials. The results obtained can be used for a more precise design of air filter structures for internal combustion engines of cars and trucks, special vehicles and working machines

depending on the expected conditions of use and, in particular, on the concentration of dust in the air.

Fibre filtration materials are characterized by the fact that the three basic parameters of the filtration process: filtration efficiency, filtration accuracy and flow resistance are closely linked. Changing the structure of the filter bed as a result of the retention and accumulation of dust mass results in an increase in filtration efficiency, a reduction in the size of dust grains in the purified air, but also results in an inevitable increase in flow resistance that is detrimental to engine operation. Fibrous materials research is directed towards the construction of a bed that has a high dust absorption capacity with minimal flow resistance, achieves high filtration efficiency and accuracy and maintains these parameters throughout the filter operation until the permissible resistance is reached. In the present work, by investigating a bed consisting of three different filter layers, which is an innovative approach in the field of filter material research, results were obtained that partly meet the above contradictory requirements. Work in this direction, using other composites given their filtration capabilities, should be continued. The results obtained can modernize methods for the design and optimization of air filtration systems in internal combustion engines.

#### Acknowledgements

This work was financed/co-financed by Military University of Technology under research project UGB 711/2024.

#### Nomenclature

CI	compression ignition	$Q_f$	air flow
$d_{pmax}$	filtration accuracy	T-PR-C	piston-piston ring-cylinder
$k_d$	mass loading of dust	$\Delta p_f$	flow resistance
$q_c$	filtration quality factor	$\varphi_f$	filtration efficiency
$q_s$	filtration efficiency index		

#### Bibliography

- [1] Alfadhli A, Alazemi A, Khorshid E. Numerical minimisation of abrasive-dust wear in internal combustion engines. *Int J Surf Sci Eng*. 2020;14:68-88. <https://doi.org/10.1504/IJSURFSE.2020.105891>
- [2] Baddocka MC, Zobeck TM, Van Pelt RS, Fredrickson EL. Dust emissions from undisturbed and disturbed, crusted playa surfaces: cattle trampling effects. *Aeolian Res*. 2011;3:31-41. <https://doi.org/10.1016/j.aeolia.2011.03.007>
- [3] Barbolini M, Di Pauli F, Traina M. Simulation der Luftfiltration zur Auslegung von Filterelementen. *MTZ*. 2014;75:52-57. <https://doi.org/10.1007/s35146-014-0556-5>
- [4] Barris MA. Total filtration<sup>TM</sup>: the influence of filter selection on engine wear, emissions, and performance. SAE Technical Paper 952557. 1995. <https://doi.org/10.4271/952557>
- [5] Bojdo N, Filippone A. A simple model to assess the role of dust composition and size on deposition in rotorcraft engines. *Aerospace*. 2019;6(44). <https://doi.org/10.3390/aerospace6040044>
- [6] Bojdo N, Filippone A. Effect of desert particulate composition on helicopter engine degradation rate. 40<sup>th</sup> European Rotorcraft Forum, Southampton. Conference Paper. September 2014. <https://doi.org/10.13140/2.1.2959.8086>
- [7] Bugli N. Automotive engine air cleaners – performance trends. SAE Technical Paper 2001-01-1356. 2001. <https://doi.org/10.4271/2001-01-1356>
- [8] Cai R-R, Li S-Z, Zhang L-Z, Lei Y. Fabrication and performance of a stable micro/nano composite electret filter for effective PM2.5 capture. *Sci Total Environ*. 2020;138297. <https://doi.org/10.1016/j.scitotenv.2020.138297>
- [9] Cardozo JIH, Sánchez DFP. An experimental and numerical study of air pollution near unpaved roads. *Air Qual Atmos Hlth*. 2019;12:471-489. <https://doi.org/10.1007/s11869-019-00678-9>
- [10] Dziubak T. Experimental study of a powercore filter bed operating in a two-stage system for cleaning the inlet air of internal combustion engines. *Energies*. 2023;16:3802. <https://doi.org/10.3390/en16093802>
- [11] Dziubak T. Properties of material with nanofiber layer used for filtering the inlet air of internal combustion engines. *Combustion Engines*. 2019;177(2):66-75. <https://doi.org/10.19206/CE-2019-212>
- [12] Dziubak T, Dziubak SD. experimental study of filtration materials used in the car air intake. *Materials*. 2020;13(16):3498. <https://doi.org/10.3390/ma13163498>

- [13] Fujiwara F, Rebagliati RJ, Dawidowski L, Gómez D, Polla G, Pereyra V et al. Spatial and chemical patterns of size fractionated road dust collected in a megacity. *Atmos Environ*. 2011;45:1497-1505. <https://doi.org/10.1016/j.atmosenv.2010.12.053>
- [14] Fussell JC, Franklin M, Green MD, Gustafsson M, Harrison RM, Hicks W et al. A review of road traffic-derived non-exhaust particles: emissions, physicochemical characteristics, health risks, and mitigation measures. *Environ Sci Technol*. 2022;56:6813-6835. <https://doi.org/10.1021/acs.est.2c01072>
- [15] Heikkilä P, Sipilä A, Peltola M, Harlin A. Electrospun PA-66 coating on textile surfaces. *Text Res J*. 2007;77(11):64-870. <https://doi.org/10.1177/0040517507078241>
- [16] Jaroszczyk T, Pardue BA, Heckel SP, Kallsen KJ. Engine air cleaner filtration performance – theoretical and experimental background of testing. Proceedings of the AFS Fourteenth Annual Technical Conference and Exposition, Tampa, 1 May 2001. Session 16.
- [17] Jaroszczyk T, Petrik S, Donahue K. Recent development in heavy duty engine air filtration and the role of nanofiber filter media. *Journal of KONES – Powertrain and Transport*. 2009;16(4):207-216.
- [18] Jiang D, Zhang W, Liu J, Geng W, Ren Z. Filtration and regeneration behavior of polytetrafluoroethylene membrane for dusty gas treatment. *Korean J Chem Eng*. 2008;25:744-753. <https://doi.org/10.1007/s11814-008-0122-2>
- [19] Jung U, Choi S-S. Classification and characterization of tire-road wear particles in road dust by density. *Polymers*. 2022; 14:1005. <https://doi.org/10.3390/polym14051005>
- [20] Kanageswari SV, Tabil LG, Sokhansanj S. Dust and particulate matter generated during handling and pelletization of herbaceous biomass: a review. *Energies*. 2022;15:2634. <https://doi.org/10.3390/en15072634>
- [21] Karczewski M. Evaluation of the diesel engine feed by unified battlefield fuel F-34/F-35 mixed with biocomponents. *Combustion Engines*. 2019;178(3):240-246. <https://doi.org/10.19206/CE-2019-342>
- [22] Kreider ML, Panko JM, McAtee BL, Sweet LI, Finley BL. Physical and chemical characterization of tire-related particles: comparison of particles generated using different methodologies. *Sci Total Environ*. 2010;408:652-659. <https://doi.org/10.1016/j.scitotenv.2009.10.016>
- [23] Leung WW-F, Curie Hau CW-Y, Choy H-F. Microfiber-nanofiber composite filter for high-efficiency and low pressure drop under nano-aerosol loading. *Sep Purif Technol*. 2018; 206:26-38. <https://doi.org/10.1016/j.seppur.2018.05.033>
- [24] Li B, Cao R, He H-D, Peng Z-R, Qin H, Qin Q. Three-dimensional diffusion patterns of traffic-related air pollutants on the roadside based on unmanned aerial vehicles monitoring. *Build Environ*. 2022;219:109159. <https://doi.org/10.1016/j.buildenv.2022.109159>
- [25] Lippi M, Riva L, Caruso M, Punta C. Cellulose for the production of air-filtering systems: a critical review. *Materials*. 2022;15:976. <https://doi.org/10.3390/ma15030976>
- [26] Liu X, Shen H, Nie X. Study on the filtration performance of the baghouse filters for ultra-low emission as a function of filter pore size and fiber diameter. *Int J Env Res Pub He*. 2019;16(2):247. <https://doi.org/10.3390/ijerph16020247>
- [27] Long J, Tang M, Liang Y, Hu J. Preparation of fibrillated cellulose nanofiber from lyocell fiber and its application in air filtration. *Materials*. 2018;11(8):1313. <https://doi.org/10.3390/ma11081313>
- [28] Long J, Tang M, Sun Z, Liang Y, Hu J. Dust loading performance of a novel submicro-fiber composite filter medium for engine. *Materials*. 2018;11:2038. <https://doi.org/10.3390/ma11102038>
- [29] Melzer HH, Brox W. Ansauggerauschdampfer und Luftfilter für BMW 524 td. *MTZ*. 1984;45:223-227.
- [30] Michalski J, Woś P. The effect of cylinder liner surface topography on abrasive wear of piston-cylinder assembly in combustion engine. *Wear*. 2011;271:582-589. <https://doi.org/10.1016/j.wear.2010.05.006>
- [31] Muschelknautz U. Design criteria for multicyclones in a limited space. *Powder Technol*. 2019;357:2-20. <https://doi.org/10.1016/j.powtec.2019.08.057>
- [32] Nowak B, Bonora M, Winnik M, Gac J. An effect of fibrous filters modification with MTMS aerogel structure on oil mist filtration dynamics. *J Aerosol Sci*. 2023;170:106147. <https://doi.org/10.1016/j.jaerosci.2023.106147>
- [33] Nyirenda G, Tamaldin N, Zakaria MH. The impact of bio-diesel blend variation contamination to engine friction, wear, performance and emission. *IJAME*. 2021;18(1):8592-8600. <https://doi.org/10.15282/ijame.18.1.2021.18.0653>
- [34] Oszczypała M, Ziółkowski J, Małachowski J. Semi-Markov approach for reliability modelling of light utility vehicles. *Eksploat Niezawodn*. 2023;25(2):161859. <http://doi.org/10.17531/ein/161859>
- [35] Owens LP, Hubbe MA. Performance factors for filtration of air using cellulosic fiber-based media: a review. *BioResources*. 2023;18(1):2440-2519. <http://doi.org/10.15376/biores.18.1.Owens>
- [36] Panko J, Kreider M, Unice K. Review of tire wear emissions. Non-exhaust emissions. Chapter 7 – Review of tire wear emissions: a review of tire emission measurement studies: identification of gaps and future needs. 2018;147-160. <http://doi.org/10.1016/b978-0-12-811770-5.00007-8>
- [37] Rieger M, Hettkamp P, Löhl T, Madeira PMP. Efficient engine air filter for tight installation spaces. *ATZ Heavy Duty Worldw*. 2019;12(2):56-59. <https://doi.org/10.1007/s41321-019-0023-9>
- [38] Schaeffer JW, Olson LM. Air filtration media for transportation applications. *Filtr Sep*. 1998;35(2):124-129. [https://doi.org/10.1016/S0015-1882\(97\)80292-3](https://doi.org/10.1016/S0015-1882(97)80292-3)
- [39] Smialek JL, Archer FA, Garlick RG. Turbine airfoil degradation in the Persian GulfWar. *JOM-J Min Met Mat S*. 1994;46(12):39-41. <https://doi.org/10.1007/BF03222663>
- [40] Summers CE. The physical characteristics of road and field dust. *SAE Technical Paper 250010*. 1925. <https://doi.org/10.4271/250010>
- [41] Świdorski A, Borucka A, Jacyna-Golda I, Szczepański E. Wear of brake system components in various operating conditions of vehicle in the transport company. *Eksploat Niezawodn*. 2019;21(1):1-9. <https://doi.org/10.17531/ein.2019.1.1>
- [42] Thomas J, West B, Huff S. Effect of air filter condition on diesel vehicle fuel economy. *SAE Technical Paper 2013-01-0311*. 2013. <https://doi.org/10.4271/2013-01-0311>
- [43] Thorpe A, Harrison RH. Sources and properties of non-exhaust particulate matter from road traffic: a review. *Sci Total Environ*. 2008;400:270-282. <https://doi.org/10.1016/j.scitotenv.2008.06.007>
- [44] Tian X, Ou Q, Liu J, Liang Y, Pui DYH. Particle loading characteristics of a two-stage filtration system. *Sep Purif Technol*. 2019;215:351-359. <https://doi.org/10.1016/j.seppur.2019.01.033>
- [45] Treuhaft MB. The use of radioactive tracer technology to measure engine ring wear in response to dust ingestion. *SAE Technical Paper 930019*. 1993. <https://doi.org/10.4271/930019>
- [46] Wang J, Kim SC, Pui DYH. Figure of merit of composite filters with micrometer and nanometer fibers. *Aerosol Sci Tech*. 2008;42:722-728. <https://doi.org/10.1080/02786820802249133>

- [47] Worek J, Badura X, Białas A, Chwiej J, Kawon K, Styszko K. Pollution from transport: detection of tyre particles in environmental samples. *Energies*. 2022;15:2816. <https://doi.org/10.3390/en15082816>
- [48] Wróblewski P. Analysis of torque waveforms in two-cylinder engines for ultralight aircraft propulsion operating on 0W-8 and 0W-16 oils at high thermal loads using the diamond-like carbon composite coating. *SAE Int J Engines*. 2022;15:129-146. <https://doi.org/10.4271/03-15-01-0005>
- [49] Xu H, Jin W, Luo J, Wang F, Zhu H, Liu G et al. Study of the PTFE multi-tube high efficiency air filter for indoor air purification. *Process Saf Environ*. 2021;151:28-38. <https://doi.org/10.1016/j.psep.2021.05.007>
- [50] Young JM, Kelly TM, Vance L. Determination of size fractions and concentrations of airborne particulate matter generated from construction and demolition waste processing facilities. *Air Qual Atmos Hlth*. 2008;1:91-100. <https://doi.org/10.1007/s11869-008-0015-x>
- [51] Ziółkowski J, Lęgas A, Szymczyk E, Małachowski J, Oszcypała M, Szkutnik-Rogoż J. Optimization of the delivery time within the distribution network, taking into account fuel consumption and the level of carbon dioxide emissions into the atmosphere. *Energies*. 2022;15(14):5198. <https://doi.org/10.3390/en15145198>

Prof. Tadeusz Dziubak, DSc., DEng. – Faculty of Mechanical Engineering, Military University of Technology, Warsaw, Poland.  
e-mail: [tadeusz.dziubak@wat.edu.pl](mailto:tadeusz.dziubak@wat.edu.pl)

